

## Spectroscopic Studies on Adsorbed Metal Carbonyls. Part 2.† Interaction of $[\text{Ru}_3(\text{CO})_{12}]$ with Silica, Titania, and Alumina ‡

John Evans\* and Gregory S. McNulty

Department of Chemistry, The University, Southampton SO9 5NH

The reactions between  $[\text{Ru}_3(\text{CO})_{12}]$  and  $\text{SiO}_2$ ,  $\text{TiO}_2$ , and  $\text{Al}_2\text{O}_3$  have been studied by electronic and i.r. spectroscopy using  $^{13}\text{C}$  isotopic substitution. The complex  $[\text{Ru}_3(\mu\text{-H})(\text{CO})_{10}(\mu\text{-OSi}\equiv)]$  was initially generated on silica, but this oxidised in air to  $[\text{Ru}^{\text{II}}(\text{CO})_2]_n$  ( $n = 2$  or  $3$ ) species. Vacuum pyrolysis however generated another  $[\text{Ru}^{\text{II}}(\text{CO})_2]_n$  species where  $n \approx 1$  and some metallic ruthenium. Subsequent heating under CO generated  $\text{Ru}^{\text{III}}$  and  $\text{Ru}^{\text{IV}}$  monocarbonyl sites. The initial silica-type supported cluster was not observed on titania and alumina. The initial impregnation reactions generate similar species to the room-temperature air oxidation products on silica. The subsequent chemistry on titania is complex but evidence was obtained for four monocarbonyls on differing ruthenium centres (suggested as  $\text{Ru}^0$ ,  $\text{Ru}^{\text{II}}$ ,  $\text{Ru}^{\text{III}}$ , and  $\text{Ru}^{\text{IV}}$ ) and a bridging carbonyl site.

Since the early study of the interaction of  $[\text{Ru}_3(\text{CO})_{12}]$  (1) and silica,<sup>1</sup> supporting ruthenium clusters on oxides has received considerable attention, both in terms of catalyst synthesis<sup>2-4</sup> and characterisation of the adsorbed species.<sup>5-7</sup> Decarbonylation occurs, with possible oxidative fragmentation of the cluster induced by surface hydroxide groups. However the details of fragmentation are in doubt. We therefore set out to use the isotopic substitution and spectral simulation techniques previously employed to study the fragmentation of  $[\text{Rh}_4(\text{CO})_{12}]$  and  $[\text{Rh}_6(\text{CO})_{16}]$  on oxides<sup>8</sup> in an attempt to characterise these adsorbed species more definitely. Diffuse reflectance measurements of the electronic spectra have been applied to try to identify absorptions due to the metal-metal bonding framework.<sup>6,9</sup> Studies on a single crystal of (1) have shown that the two lowest energy electronic absorptions are associated with transitions to the  $\text{M-M } \pi^*$  orbital.<sup>10</sup> We also surveyed the electronic spectra of a series of ruthenium dimers and clusters to test whether these low-energy absorptions could be used as a guide to cluster nuclearity.

### Experimental

$[\text{Ru}_3(\text{CO})_{12}]$  was prepared by the reaction of  $\text{RuCl}_3 \cdot 3\text{H}_2\text{O}$  with CO in dry methanol.<sup>11</sup> Electronic spectra were recorded on a Perkin-Elmer 554 spectrophotometer either in transmission mode (for solutions) or diffuse reflectance (for oxide samples) employing  $\text{BaSO}_4$  or  $\text{MgO}$  as a standard. Other general experimental and computational procedures are described in ref. 8.

**Interaction of  $[\text{Ru}_3(\text{CO})_{12}]$  and Silica.—Solution reactions.**  $[\text{Ru}_3(\text{CO})_{12}]$  (1) (0.020 g) was dissolved in cyclohexane (35  $\text{cm}^3$ ), the system flushed with  $\text{N}_2$  and heated to reflux. Aerosil 200 (or 380) (0.200 g) was then added and the mixture refluxed with stirring. After the required reaction time, the solid was filtered off from the reaction mixture, washed with  $\text{CH}_2\text{Cl}_2$  to remove excess (1), and dried *in vacuo*. An exactly analogous reaction was carried out in n-octane solution.

**Disc pyrolysis experiments.** A sample containing species (A), produced by the reaction of (1) and Aerosil 200 in cyclohexane for 2 h, was pressed into a 14-mm diameter disc. This was mounted in a heated cell and pyrolysed under vacuum (0.1 Torr). After heating, the cell was filled with an atmos-

phere of CO and heated for the required reaction time, allowed to cool, evacuated, and the i.r. spectrum of the disc recorded in the cell.

**Powder pyrolysis experiments.** A powder sample of (A) was placed in a quartz tube fitted with a poly(tetrafluoroethylene) joint and stopcock. The sample was pyrolysed using an external heating coil while continually pumped at  $\sim 0.1$  Torr.

**$^{13}\text{C}$  Enrichment of  $[\text{Ru}_3(\text{CO})_{12}]$ .**—This was carried out by heating a solution of (1) (0.200 g) in n-octane (20  $\text{cm}^3$ ) under  $^{13}\text{C}$  at 80 °C for 15 h. Analysis of the isotopic pattern of the molecular ion in the mass spectrum of the product indicated a  $^{13}\text{C}$  level of  $35 \pm 5\%$ .

**Attempted Preparations of  $[\text{Ru}_3(\mu\text{-H})(\text{CO})_{10}(\mu\text{-OR})]$  (R = Ph or  $\text{SiPh}_3$ ).**—Complex (1) (0.025 g) was dissolved in n-octane (35  $\text{cm}^3$ ), heated to reflux under  $\text{N}_2$ , ROH (0.075 g) added, and the solution refluxed for 2 h. The solvent was removed and the products separated by t.l.c. Only unreacted (1),  $[\text{Ru}_4\text{H}_4(\text{CO})_{12}]$ , and  $[\text{Ru}_4\text{H}_2(\text{CO})_{13}]$  could be isolated. Carrying out the reaction in refluxing cyclohexane for 15 h (for R =  $\text{SiPh}_3$ ) gave rise to the same products.

**Interaction of  $[\text{Ru}_3(\text{CO})_{12}]$  and Titania or Alumina.—Solution reactions.** These were carried out as for the interaction with silica using n-pentane, hexane, cyclohexane, n-octane, and n-nonane as the reaction medium.

**Schlenk-tube reactions.** These were carried out as for the solution reactions but using conventional Schlenk apparatus. Extraction of the oxide powder was carried out under  $\text{N}_2$  and spectra recorded on samples made up in a nitrogen-filled glove bag.

**Disc pyrolysis experiments.** The procedure was similar to the silica variants, excepting that polymer discs were used to prevent the oxide adhering to the die while the oxide disc was being formed.

### Results

**$[\text{Ru}_3(\text{CO})_{12}]$  on Silica.**—After refluxing a suspension of Aerosil 200 in a solution of (1) in cyclohexane for 70 min, the oxide became orange. A single species, (A), is considered to be present, exhibiting i.r. bands at 2 107w, 2 076s, 2 066s, 2 026s, and 1 991m  $\text{cm}^{-1}$ . On standing in air and light at room temperature, species (A) decomposed to a second species (B), which exhibited two strong  $\nu(\text{CO})$  i.r. absorptions at  $\sim 2 055$  and 1 990  $\text{cm}^{-1}$  (Figure 1). This material was also orange, but on further exposure to air, it gradually turned grey. The life-

† Part 1 is ref. 8.

‡ Non-S.I. units employed: Torr = (101 325/760)  $\text{N m}^{-2}$ ; dyn =  $10^{-5}$  N.

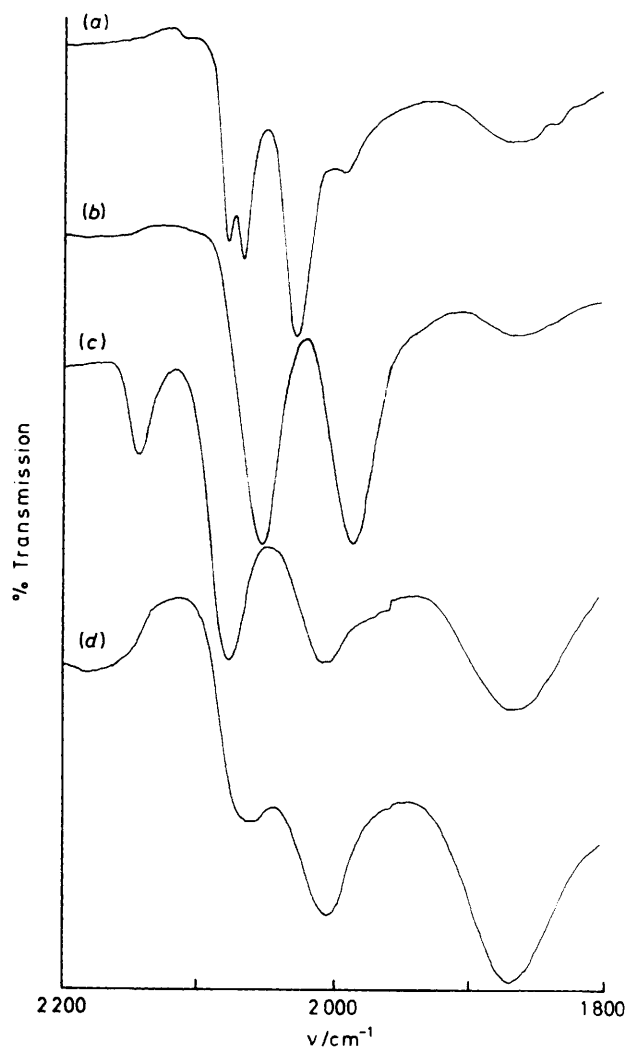


**Figure 1.** I.r. spectra of species formed from  $[\text{Ru}_3(\text{CO})_{12}]$  on  $\text{SiO}_2$ : (a) species (A), (b) species (B), (c) mixture of species (C), (D), and (E) produced by exposing a pyrolysed disc to CO, and (d) species (C) produced by powder pyrolysis experiments on (A). The band at  $\sim 1880 \text{ cm}^{-1}$  is due to the silica support

time of (A) was  $\sim 36 \text{ h}$  at room temperature and  $\sim 1 \text{ month}$  at  $-20^\circ \text{C}$ . Extending the initial reflux period to 30 h afforded a fawn oxide containing a mixture of (A) and (B). An i.r. spectrum of the reaction solution after 30 h showed absorptions due to unchanged (1),  $[\text{Ru}_4\text{H}_4(\text{CO})_{12}]$ , and  $[\text{Ru}_4\text{H}_2(\text{CO})_{13}]$ . These products were confirmed by mass spectrometry.

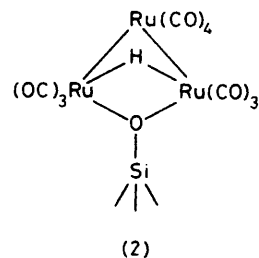
Reaction in refluxing n-octane gave similar results, excepting that (A) was rapidly formed in high concentration and after 4.5 h some decomposition to (B) occurred. After 32 h reaction time, the latter species became predominant, and the oxide darkened. On standing, the octane-produced sample of (A) decomposed more rapidly to (B), and the resulting (B)-type material was dark grey rather than orange. Aerosil 380 gave a higher surface loading, but a lower stability for species (A).

The decomposition of (A) *in vacuo* was monitored on a pressed disc by i.r. spectroscopy. This species gave i.r. bands at slightly higher frequencies ( $2112\text{vw}$ ,  $2079\text{s}$ ,  $2069\text{s}$ ,  $2034\text{s}$ , and  $2000\text{m cm}^{-1}$ ) than in the Nujol mull. Pyrolysis at  $50^\circ \text{C}$  *in vacuo* gave a gradual change to a spectrum exhibiting four i.r. bands at  $2135\text{w}$ ,  $2067\text{s}$ ,  $2045(\text{sh})$ , and  $2006 \text{ cm}^{-1}$ . Pyrolysis at  $125^\circ \text{C}$  for 6 h afforded a weak i.r. spectrum with ab-

**Table 1.** Electronic spectroscopy data for dissolved and supported ruthenium complexes

Complex	$\lambda_{\text{max.}}/\text{nm}$ ( $10^{-4}\epsilon/\text{dm}^3 \text{ mol}^{-1} \text{ cm}^{-1}$ )
$[\text{Ru}_3(\text{CO})_{12}]^a$	386(0.44), 318, 270, 235, $\sim 200(2.4)$
$[\text{Ru}_2(\eta^5\text{-C}_5\text{H}_5)_2(\text{CO})_3(\text{CCH}_2)]^a$	413(0.08), 351(0.15), 262s, 202s
$[\text{Ru}_2(\eta^5\text{-C}_5\text{H}_5)_2(\text{CO})_3(\text{CHCH}_2)\text{-BF}_4]^b$	403(sh), 312(sh), 261(sh), 239
$[\text{Ru}_2(\eta^5\text{-C}_5\text{H}_5)_2(\text{CO})_4]^a$	420(0.05), 325s, 264m, 219s, 203s
$[\text{Ru}_2(\eta^5\text{-C}_5\text{H}_5)_2(\text{CO})_3(\text{CHCH}_3)]^a$	413w, 361(0.15), 322(0.21), 263(1.11), 226(1.61), 202s
$[\text{Ru}_3\text{H}_3(\text{CO})_9(\text{CMe})]^a$	369w, 282m, 204s
$[\text{Ru}_4\text{H}_4(\text{CO})_{12}]^a$	359s, 311m, 243s, 203s
$[\text{Ru}_4\text{H}_2(\text{CO})_{13}]^a$	521vw, 415w, 352m, 252m(sh), 203s
$[\text{Ru}_5\text{C}(\text{CO})_{15}]^a$	518wm, 332mw, 221s
$[\text{Ru}_6\text{C}(\text{CO})_{17}]^a$	412w, 275m(sh), 200s
(A) (orange) <sup>c</sup>	432w(sh), 404w(sh), 324s, 253s br
(B) (orange) <sup>c</sup>	403s, 371w, 338s, 300w, 254s br
(C) (black) <sup>c</sup>	409vw, 341vw
(C) + (D) + (E) (off-white) <sup>c</sup>	421w, 359m, 299s, 278s, 238s
(C) (off-white) <sup>c</sup>	418w, 371w(sh), 301m(sh), 226s
(L) (orange) <sup>d</sup>	588vw, 405m, 372m(sh), 340s, 236s

<sup>a</sup> In cyclohexane. <sup>b</sup> In  $\text{CH}_2\text{Cl}_2$ . <sup>c</sup> On  $\text{SiO}_2$ . <sup>d</sup> On  $\text{Al}_2\text{O}_3$ .



sorptions at  $2143\text{vw}$ ,  $2074\text{m}$ , and  $2015 \text{ cm}^{-1}$ . After exposure of this sample to CO (300 Torr), at  $45^\circ \text{C}$  for 3 h, the sample exhibited  $\nu(\text{CO})$  bands at  $2140\text{w}$ ,  $2075\text{s}$ , and  $2011\text{m cm}^{-1}$ . Further such treatment increased the band intensity and slight frequency shifts to give features at  $2144\text{m}$ ,  $2076\text{s}$ , and  $2010\text{m cm}^{-1}$ . It is apparent that pyrolysis at high temperatures does not yield species (B), but appears to form two other carbonyls *viz.* (C) ( $2067$  and  $2005 \text{ cm}^{-1}$ ) and (D) ( $2136 \text{ cm}^{-1}$ ). Exposure to CO particularly increased the intensity at  $\sim 2075 \text{ cm}^{-1}$  and this is assigned to a fifth species, (E) (Figure 1). A similar pattern of behaviour was observed by the pyrolysis of the powdered sample containing (A).

Diffuse reflectance spectra of some of these materials were recorded and the results are presented in Table 1. In addition the electronic spectra of some polynuclear ruthenium complexes were recorded and are also included in Table 1. While it is clear that all the complexes exhibit absorptions near to or at lower energies than the two metal-metal chromophores of  $[\text{Ru}_3(\text{CO})_{12}]$  at 386 and 318 nm, it is also clear that there is no simple correlation with cluster nuclearity. The specific nature of each complex has a marked effect on the energies of the lower lying electronic transitions.

*Identification of species (A)–(E).* The relatively sharp  $\nu(\text{CO})$  absorptions, colour, and electronic absorptions of (A) are consistent with the cluster being intact in this species. Indeed the recent proposal is a grafted molecular cluster,  $[\text{Ru}_3(\mu\text{-H})(\text{CO})_{10}(\mu\text{-OSi}\equiv)]$  (2),<sup>7</sup> and seems soundly based. Attempts

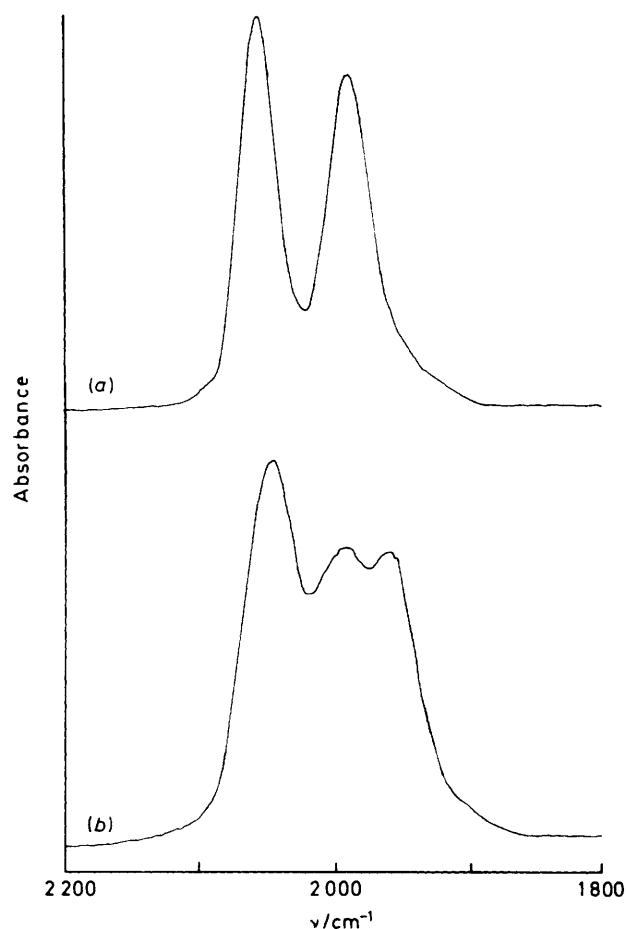
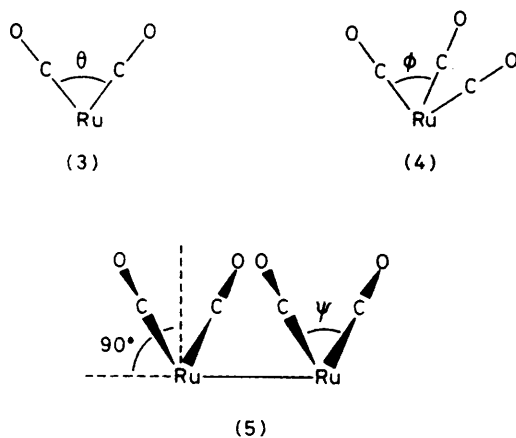


Figure 2. Background subtracted spectra showing species (B) on silica; (a) natural abundance and (b)  $^{13}\text{C}$  enriched



were made to synthesise close analogues of (A) by the reaction of  $[\text{Ru}_3(\text{CO})_{12}]$  with  $\text{PhOH}$  and  $\text{SiPh}_3(\text{OH})$ . It is interesting that both these model reactions and the interaction of (1) with silica generated  $[\text{Ru}_4\text{H}_4(\text{CO})_{12}]$  and  $[\text{Ru}_4\text{H}_2(\text{CO})_{13}]$ . It is also clear that the different conditions used in this and the earlier work of Robertson and Webb<sup>1</sup> means that there is not a direct correlation between their set of five species and ours; their species (A) is very probably a physisorbed dispersion of  $[\text{Ru}_3(\text{CO})_{12}]$ .

Exposure of (A) to air generated a second orange material

Table 2. Parameters used to model the species (B) on silica. Plotting linewidths of  $36\text{ cm}^{-1}$  were used for the  $^{13}\text{C}$ -enriched spectrum

Model	Angle ( $^\circ$ )	Force constants ( $\text{mdyn \AA}^{-1}$ )	$^{13}\text{C}$ (%)
$\text{C}_{2v}, \text{M}(\text{CO})_2$	$\theta = 90$	$K = 16.506$ $k_1 = 0.539$	32
$\text{C}_{3v}, \text{M}(\text{CO})_3$	$\phi = 75.5$	$K = 16.326$ $k_1 = 0.359$	40
$\text{C}_{2v}, [\text{M}(\text{CO})_2]_2$	$\psi = 90$	$K = 16.45$ $k_{\text{gem}} = 0.46$ $k_{\text{cis}} = 0.057$ $k_{\text{trans}} = 0.078$	32

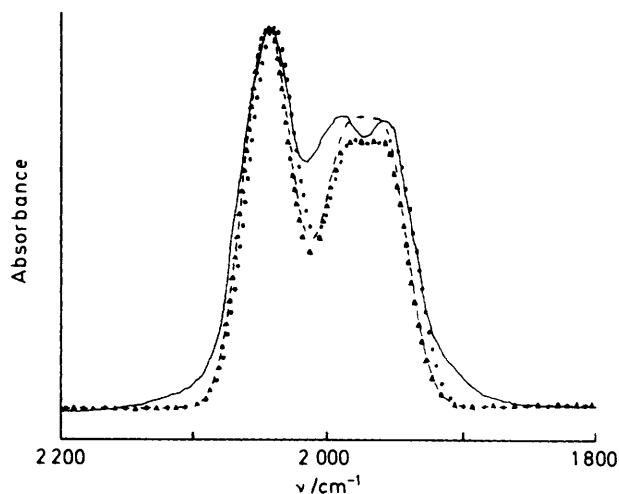


Figure 3. Modelling studies of the  $\nu(\text{CO})$  bands of the  $^{13}\text{C}$ -enriched sample of (B); (—) experimental spectrum, (---) computed using a  $\text{M}(\text{CO})_2$  model, (···) a  $\text{M}(\text{CO})_3$  model, and ( $\blacktriangle\blacktriangle$ ) a  $[\text{M}(\text{CO})_2]_2$  model

(B) as an intermediate to the grey material reported previously.<sup>1</sup> The relative intensities of the two  $\nu(\text{CO})$  bands do not vary under changing experimental conditions, suggesting that both can be assigned to a single species. The relative intensities of these two bands, the colour, and the u.v.-visible absorption spectrum suggest a  $[\text{Ru}(\text{CO})_2]_n$  ( $n > 1$ ) type moiety.

Species (B) was generated from a  $35 \pm 5\%$   $^{13}\text{C}$ -enriched sample of  $[\text{Ru}_3(\text{CO})_{12}]$  and exhibited  $\nu(\text{CO})$  absorptions at  $2048\text{s}$ ,  $1994\text{m}$ , and  $1964\text{m cm}^{-1}$ . This immediately discounted the possibility that (B) is a pair of monocarbonyls, since bands due to the full isotopic shift would be expected at  $\sim 2008$  and  $1944\text{ cm}^{-1}$ . Background subtracted versions of the spectra of the natural abundance and  $^{13}\text{C}$ -enriched samples of species (B) are presented in Figure 2. The lower frequency  $\nu(\text{CO})$  absorption of the natural abundance sample has a non-Gaussian profile. Although its integrated intensity is slightly larger (1.14 : 1), as a compromise between this and the observed peak height, these bands were assumed to have equal intensity. Three models,  $\text{Ru}(\text{CO})_2$  (3) ( $\theta = 90^\circ$ ),  $\text{Ru}(\text{CO})_3$  (4) ( $\phi = 75.5^\circ$ ), and a  $\text{Ru}_2(\text{CO})_4$  unit ( $\psi = 90^\circ$ ) (5) could all be fitted to the natural abundance spectrum using the parameters in Table 2. Comparisons between the computed and experimental spectra of the  $^{13}\text{C}$ -enriched sample of species (B) are presented in Figure 3. All three models give reasonable, rather than good, intensity matches. The tricarbonyl model (4) is considered unlikely for two reasons, *viz.* the small bond angle and high value of the  $^{13}\text{C}$  incorporation that it requires.

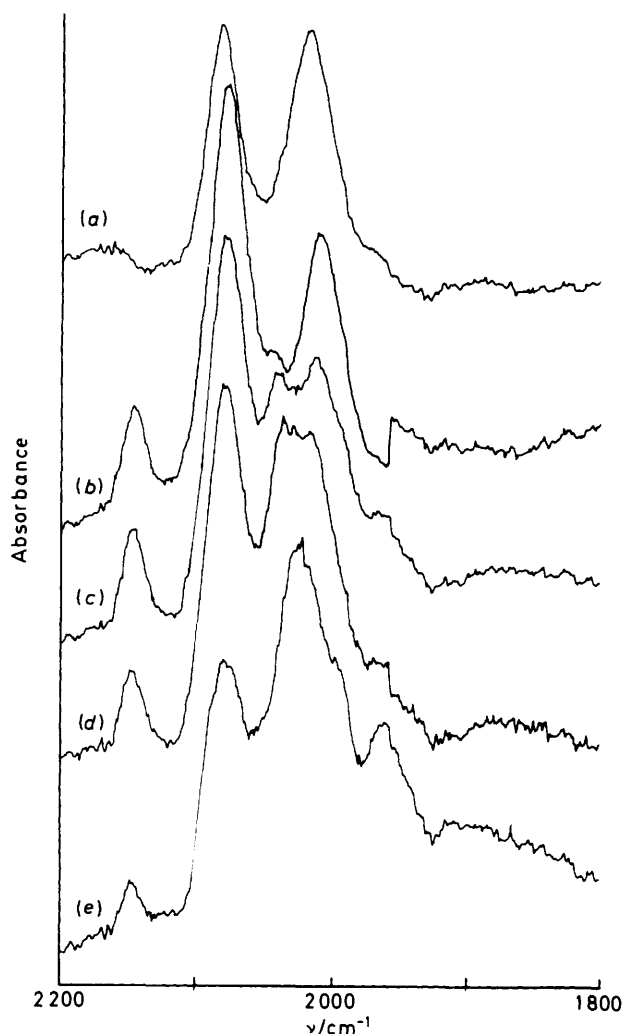


Figure 4. Background subtracted i.r. spectra on silica; (a) species (C); (b) species (C) +  $^{12}\text{CO}$  (500 Torr, 130 °C, 24 h) to give a mixture of (C) + (D) + (E); and (c), (d), and (e) show these species with an increasing  $^{13}\text{CO}$  content

Observation of the low-energy electronic transitions favours the  $[\text{M}(\text{CO})_2]_n$  ( $n = 2$ ) model, but it is also possible that (B) contains a higher oligomer ( $n \geq 3$ ). Calculations of more complex models would, however, require too many assumptions to be of much value.

A powdered sample containing species (A) on Aerosil 200 was pyrolysed at 200 °C *in vacuo* for 15 h. The resulting very pale grey material exhibited two  $\nu(\text{CO})$  absorptions at 2078 and 2014  $\text{cm}^{-1}$  (relative intensities 1:1.2) corresponding largely to species (C). Interaction of (C) with  $^{12}\text{CO}$  and then  $^{13}\text{CO}$  was carried out and the i.r. spectra of the resulting species shown in Figure 4. The initial reaction of (C) with  $^{12}\text{CO}$  (500 Torr) for 24 h at 130 °C generated an off-white sample with i.r. bands at 2144w, 2075s, and 2009ms  $\text{cm}^{-1}$  [due to species (C), (D), and (E)]. This material was then reacted with  $^{13}\text{CO}$  (500 Torr) for 3 h at 130 °C, giving rise to the i.r. spectrum (e) in Figure 4. Finally, in the remaining two spectra, (c) and (d), the  $^{13}\text{CO}$  was gradually replaced by  $^{12}\text{CO}$ . The spectra containing the isotope mixtures exhibit no intensity between 2144 and 2075  $\text{cm}^{-1}$ , but as the  $^{13}\text{CO}$  proportion is increased, the intensity of the high-frequency band is reduced and a high-frequency shoulder is observable on the band at 2075  $\text{cm}^{-1}$ .

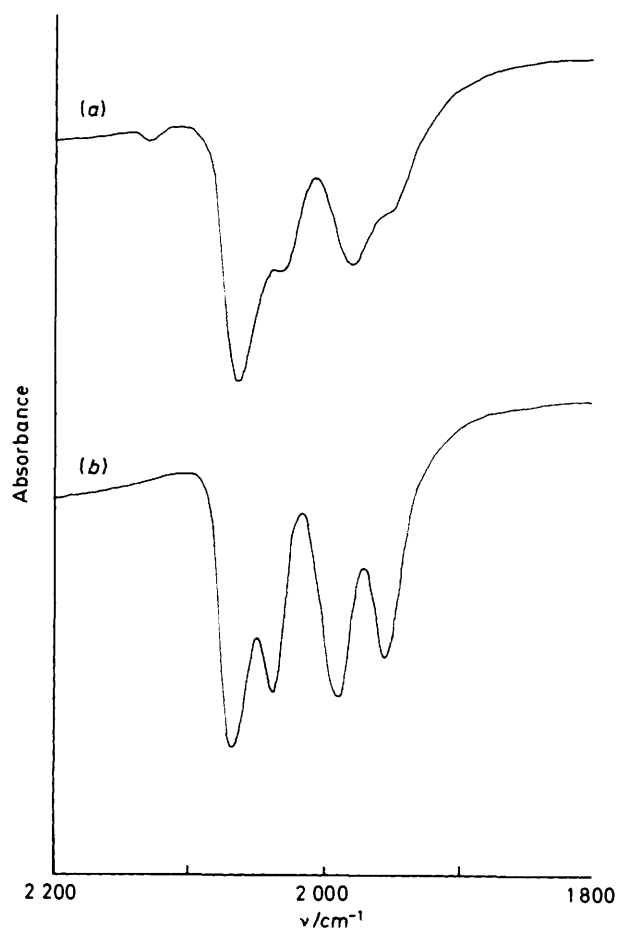
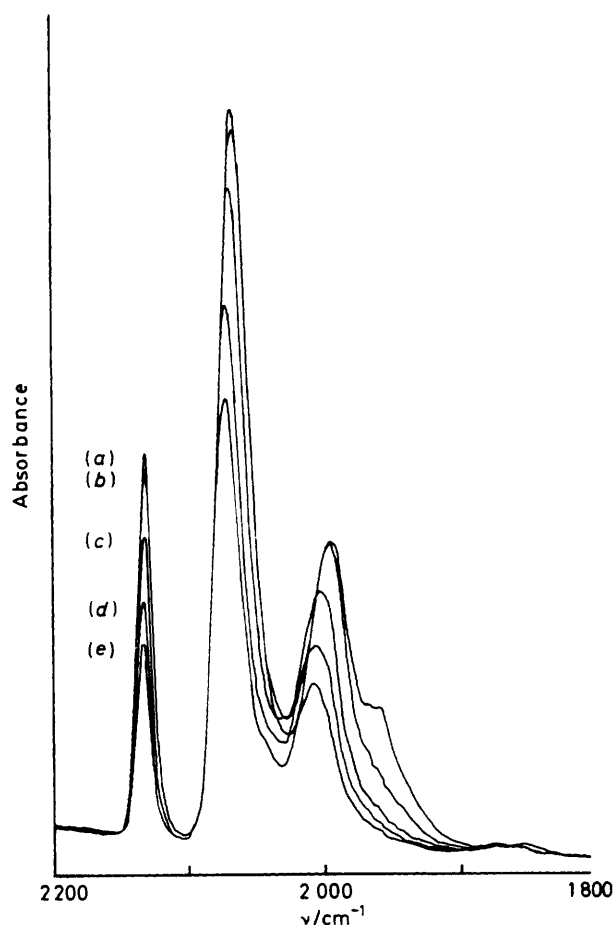


Figure 5. I.r. spectra of species formed by the reaction of  $[\text{Ru}_3(\text{CO})_{12}]$  and titania; (a) reaction in cyclohexane for 70 min and (b) reaction in nonane for 3 h

The full  $^{13}\text{CO}$  isotopic shift would transfer the band at 2144  $\text{cm}^{-1}$  to 2096  $\text{cm}^{-1}$ , corresponding to the shoulder positions. The band at 2144  $\text{cm}^{-1}$  is therefore assigned as due to species (D), a Ru-CO species in an oxidised site. This means that the extra intensity at  $\sim 2075 \text{ cm}^{-1}$  observed after treating (C) with CO is due to another species (E), also a Ru-CO unit, probably in a lower oxidation state than (D). As such, (D) would be expected to show a single  $^{13}\text{CO}$  i.r. absorption at  $\sim 2027 \text{ cm}^{-1}$ . The spectrum obtained with the highest  $^{13}\text{CO}$  content [Figure 4(e)] contains a prominent peak at 2025  $\text{cm}^{-1}$ , due to this band superimposed on those of (C). Species (C) itself has the attributes of another  $[\text{Ru}(\text{CO})_2]_n$  moiety. It acts as a weak chromophore in the visible region, but in addition, is co-existent with a black material, probably metallic ruthenium. Weak i.r. features near 2040  $\text{cm}^{-1}$  may be due to terminal sites on the metallic ruthenium.<sup>7</sup>

$[\text{Ru}_3(\text{CO})_{12}]$  on Titania.—The product obtained by interacting titania and a solution of (1) in refluxing hexane for 40 min exhibited a pale orange colouration and  $\nu(\text{CO})$  bands at 2058m, 2033mw, 1981mw, and 1949w  $\text{cm}^{-1}$ . Similar results were obtained under normal and Schlenk apparatus. After 4 h reaction time an additional weak high-frequency feature was observed in the spectrum of the isolated oxide [2131vw, 2064ms, 2035m(sh), 1980m, and 1951(sh)  $\text{cm}^{-1}$ ] and extending the reaction time to 25 h afforded a darkened oxide with a similar, but weaker and broader i.r. spectrum. The use of



**Figure 6.** I.r. spectra of the vacuum pyrolysis experiment (ii), carried out at 90 °C on a TiO<sub>2</sub> supported sample from (i) previously exposed to CO. Reaction times (min): (a) 0, (b) 10, (c) 20, (d) 30, and (e) 40

cyclohexane as solvent gave almost identical results. After 70 min reaction time, the titania became pale orange and exhibited i.r. bands at 2 132w, 2 062vs, 2 031s, 1 981s, and 1 951(sh) cm<sup>-1</sup> [Figure 5(a)]. After 18 h reflux, the orange-brown product exhibited a broadened version of this spectrum. However after 1 h reflux in n-octane the product was fawn and showed three ν(CO) absorptions at 2 132mw, 2 075vs, and 1 983vs cm<sup>-1</sup>. After 6 h, the grey oxide similarly showed a three-band spectrum (2 132w, 2 068vs, and 1 990vs cm<sup>-1</sup>) and extending the reaction time up to 18 h yielded a dark grey material which gave a weaker i.r. spectrum with bands at 2 067 and 1 990s cm<sup>-1</sup>. A fawn product was also obtained by using n-nonane as the reflux solvent after 3 h, with i.r. bands at 2 130vw, 2 065vs, 2 035vs, 1 992vs, 1 984vs, and 1 956s cm<sup>-1</sup>. On repeating this experiment, the bands at 1 992 and 1 984 cm<sup>-1</sup> were not resolved [Figure 5(b)].

Four disc pyrolysis experiments (i)—(iv) were carried out to try to establish the components of these complex products.

(i) A disc formed from the reaction product of [Ru<sub>3</sub>(CO)<sub>12</sub>] with TiO<sub>2</sub> in cyclohexane was pyrolysed *in vacuo* at 70 °C for 70 min. The disc of this product exhibited broadening of the bands when compared with mull spectra (2 133w, 2 075vs, and 1 993s br cm<sup>-1</sup>). Pyrolysis at 70 °C gave an initial loss of intensity in the 2 000—1 970 cm<sup>-1</sup> region which was accompanied by intensity loss at ~2 065 cm<sup>-1</sup>. After 125 min, the disc showed three fairly sharp bands at 2 135w, 2 078vs,

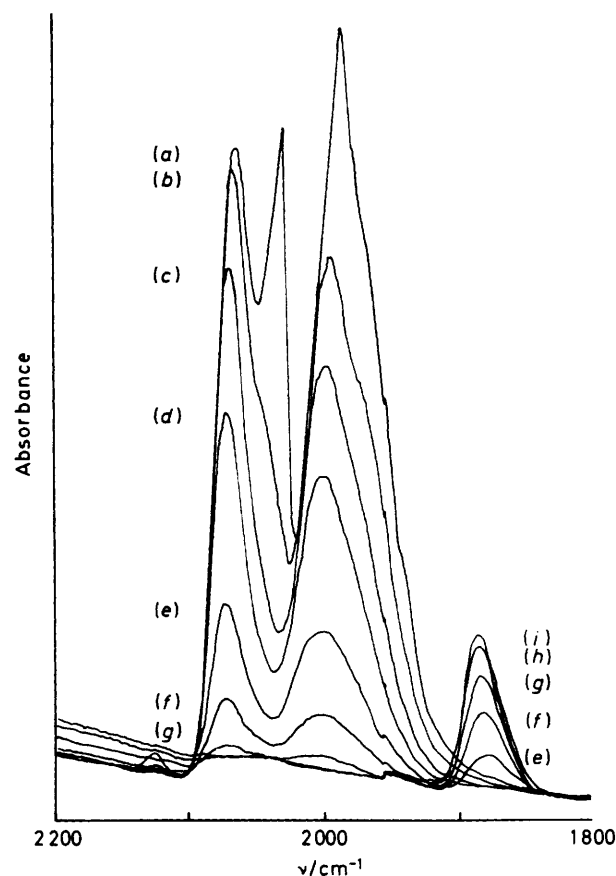


**Figure 7.** I.r. spectra showing the vacuum pyrolysis experiment at 150 °C (iii) on titania. Reaction times: (a) 0, (b) 10, (c) 20, (d) 30, (e) 40, (f) 50, (g) 60, (h) 70, and (i) 80

and 2 010m cm<sup>-1</sup> together with a broad weak absorption at ~1 875 cm<sup>-1</sup>. Treatment with CO (300 Torr) at 70 °C for 140 min then afforded a sample with i.r. bands at 2 136vs, 2 073vs, 1 998s, and 1 962m cm<sup>-1</sup>.

(ii) Pyrolysis of the disc from (i) at 90 °C gave similar observations to pyrolysis (i), in that there was an immediate intensity loss of the band at 1 962 cm<sup>-1</sup> accompanied by losses at ~2 060 and 1 990 cm<sup>-1</sup>. This resulted in a product showing ν(CO) absorptions at 2 136s, 2 077vs, and 2 011m cm<sup>-1</sup> after ~40 min (Figure 6).

(iii) Pyrolysis at 150 °C of the sample formed by the reaction of (1) and TiO<sub>2</sub> in nonane for 3 h gave a disc whose spectrum exhibited bands at 2 130w, 2 072vs, 2 035vs, 1 993vs, and 1 940br(sh) cm<sup>-1</sup>. Pyrolysis caused rapid intensity loss for the band at 2 035 cm<sup>-1</sup> and in the 2 000—1 940 cm<sup>-1</sup> region (Figure 7). After 1 h the growth of a band at 1 886 cm<sup>-1</sup> was observed.

(iv) Pyrolysis of the initial sample as in (iii) at 55 °C, gave, as previously observed a spectrum with principal intensity losses below 2 000 cm<sup>-1</sup> and from the band at ~2 039 cm<sup>-1</sup>. At this temperature, the final spectrum still showed strong ν(CO) bands at 2 069, 1 995, and 1 973 cm<sup>-1</sup>. This sample was then pyrolysed at 100 °C for 15 h followed by heating at 140 °C for 4 h, resulting in an i.r. spectrum with three principal absorptions at 2 070s, 2 000s br, and 1 873m cm<sup>-1</sup>. Exposure to CO (150 Torr) for 5 min at room temperature produced additional features [ν(CO) at 2 130vw, 2 070s, 1 998s, 1 978s, and 1 873m cm<sup>-1</sup>] which gained intensity on longer reaction times (2 130m, 2 070s, 1 998s, and 1 873m cm<sup>-1</sup>). Heating this last sample with

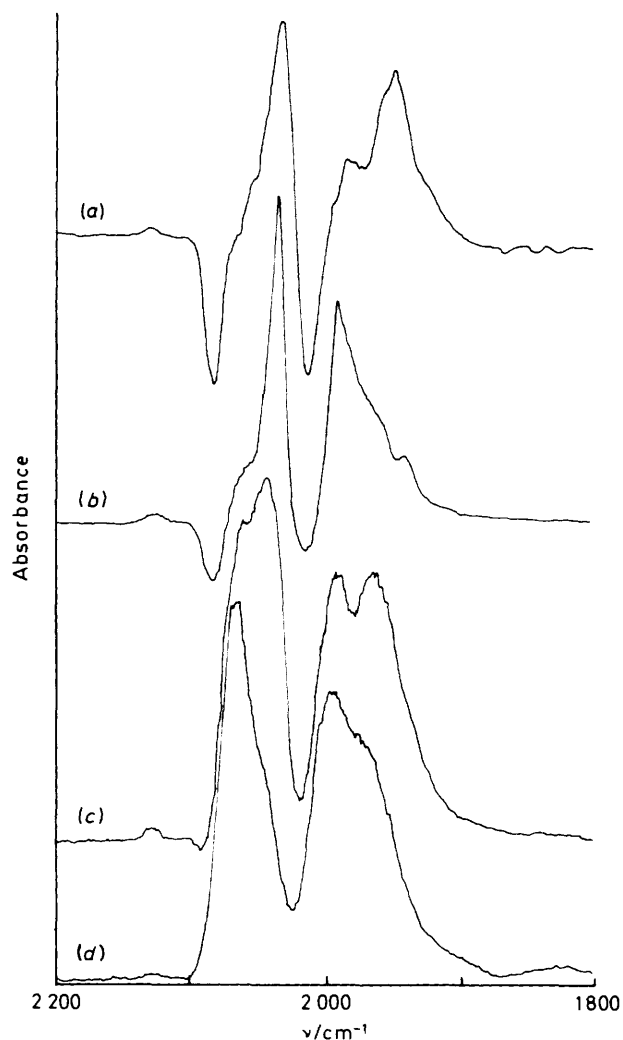


**Figure 8.** I.r. difference spectra showing changes through the  $\text{TiO}_2$  disc pyrolysis experiments. A positive absorbance represents a loss of intensity and a negative displacement a gain through the reaction period. (a) experiment (iv) (at  $55^\circ\text{C}$ ), 40–145 min; (b) (iii) (at  $150^\circ\text{C}$ ), 0–10 min; (c) (iii), 10–20 min; and (d) (iii), 20–30 min

$\text{CO}$  (150 Torr) at  $45^\circ\text{C}$  for 15 h produced a similar i.r. spectrum to that in (i) after that sample was exposed to  $\text{CO}$  [ $\nu(\text{CO})$  at  $2135\text{m}$ ,  $2070\text{s}$ ,  $1998\text{s}$ ,  $1966\text{s}(\text{sh})$ , and  $1870\text{m}$   $\text{cm}^{-1}$ ].

Identification of the bands due to particular species was possible after careful analysis of the disc pyrolysis results.

(a) A direct subtraction of the spectrum obtained after 145 min from that obtained after 40 min [Figure 8(a)] in experiment (iv) results in a loss of bands at  $2034$  and  $1951$   $\text{cm}^{-1}$  (relative intensities 1.0 : 1.075) [species (F)], together with higher frequency shoulders. However, examination of the difference spectra at the beginning of the higher temperature run (iii) [Figure 8(b)] shows only a sharp intensity loss at  $2034$   $\text{cm}^{-1}$  (together with a reduction at  $\sim 1990$   $\text{cm}^{-1}$ ) indicating that (F) is made up of two components *viz.* ( $F_1$ ) ( $2034$   $\text{cm}^{-1}$ ) and ( $F_2$ ) ( $1951$   $\text{cm}^{-1}$ ).

(b) The difference spectrum in Figure 8(a) shows gains in intensity at  $2080$  and  $2012$   $\text{cm}^{-1}$  (relative intensities 0.475 : 0.449) due to (G) being formed as (F) is lost. In experiment (iii), (G) exhibited bands at  $2077$  and  $2005$   $\text{cm}^{-1}$ , corresponding to the higher frequency pair of peaks evident by considering the difference spectra (c) and (d) in Figure 8.

(c) The second species is evident in these latter two spectra as being lost significantly between 10 and 20 min of pyrolysis at  $150^\circ\text{C}$ , (iii), shows i.r. absorptions at  $2050$ – $2044$  and  $1975$ – $1968$   $\text{cm}^{-1}$ , and is labelled (H).

(d) It is evident from Figure 7 that a species is formed at  $150^\circ\text{C}$  exhibiting a single broad band at  $1886$   $\text{cm}^{-1}$  [species (I)].

(e) The respective rates of intensity loss observed in Figure 6 [experiment (iii)] suggest that some of the band at  $\sim 2070$   $\text{cm}^{-1}$  is due to another species since the intensity of the band at  $\sim 2000$   $\text{cm}^{-1}$  would reach zero before that of the  $2070$   $\text{cm}^{-1}$  absorption. In addition, experiment (iii) shows these two bands to be of approximately equal intensity, although in this instance a strong band at  $\sim 2135$   $\text{cm}^{-1}$  is not observed. Consideration of the spectra in (ii) which show initial intensity loss at  $\sim 2138$   $\text{cm}^{-1}$  which is not matched at  $2070$   $\text{cm}^{-1}$ , and the relative intensities of the three bands of the final spectrum of experiment (i) ( $\sim 2135\text{w}$ ,  $\sim 2075\text{s}$ , and  $\sim 2010\text{m}$   $\text{cm}^{-1}$ ) indicate that there are two further distinct species with bands at  $2135$   $\text{cm}^{-1}$  (J) and  $2070$   $\text{cm}^{-1}$  (K).

**Identification of species (F)–(K).** On the basis of these results, it appears that the product of the reaction between  $[\text{Ru}_3(\text{CO})_{12}]$  and  $\text{TiO}_2$  in refluxing cyclohexane, which yields the spectrum in Figure 5(a), contains the species (G), (H) and, in smaller quantities, (J). At high reflux temperatures, in nonane, (J) is in very small abundance and there is relatively a larger proportion of species (H). [This could also be due to species ( $F_1$ ) and ( $F_2$ ).]

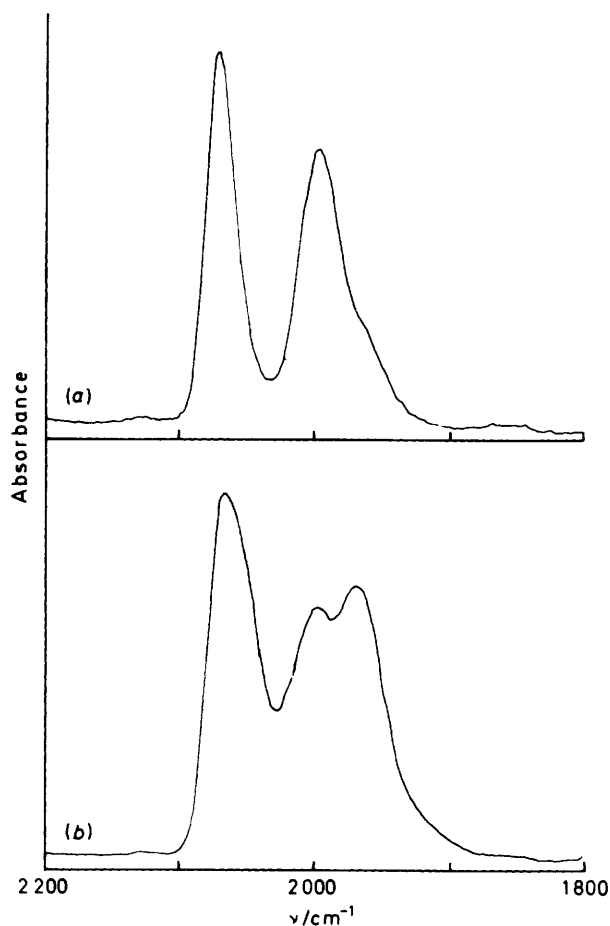
The complexity of this system precluded a full isotopic study, however the materials generated on prolonged exposure to air were spectroscopically less difficult. These materials were blue-green and exhibited two  $\nu(\text{CO})$  bands at  $\sim 2062$  and  $1985$   $\text{cm}^{-1}$ . A similar material is formed by the reaction between (I) and  $\text{TiO}_2$  in *n*-octane for 20 h. In this case the  $\nu(\text{CO})$  bands were at slightly higher frequencies ( $2071$  and  $1996$   $\text{cm}^{-1}$ ) and relative intensities 1 : 1.2, with the latter band showing a low-frequency tail indicative of another absorption. The spectra of the natural abundance and  $^{13}\text{C}$ -enriched versions of this sample are shown in Figure 9. The natural abundance spectrum was considered to consist of three Gaussian peaks at  $2071$ ,  $1996$ , and  $\sim 1960$   $\text{cm}^{-1}$ , of relative intensities 1 : 0.87 : 0.25, although the high-frequency band could be due to two components. The peak positions appear to indicate the presence of (G) and (H) and/or ( $F_2$ ). The support absorbed strongly below  $\sim 420$  nm, but a weak broad electronic absorption was observed at  $590$  nm, perhaps suggesting some oligomerisation. Comparison with results reported for the  $[\text{Ru}_3(\text{CO})_{12}]$  on alumina system<sup>6</sup> suggests that (G) is a mononuclear dicarbonyl and (H) is a polynuclear dicarbonyl. Model spectra were synthesised for three possibilities: (i) (G) as  $\text{Ru}(\text{CO})_2$  (3) with ( $F_2$ ) as  $\text{Ru}-\text{CO}$  (6); (ii) (G) as  $[\text{Ru}(\text{CO})_2]_2$  (5) with ( $F_2$ ) as (6); and (iii) (G) as (3) with (H) as (5). The parameters used are presented in Table 3. All three models could be used to fit the natural abundance spectrum, but discrimination was possible on the basis of the  $^{13}\text{C}$ -enriched results (Figure 10). Model (i) gives a relatively poor fit, and overall, that of model (iii) is the most successful.

Tentative suggestions at this stage are that species ( $F_1$ ), ( $F_2$ ), (J), and (K) may contain  $\text{Ru}-\text{CO}$  units, (G) may contain  $\text{Ru}(\text{CO})_2$ , (H)  $[\text{Ru}(\text{CO})_2]_2$ , and (I) a  $\text{Ru}_2(\text{CO})$  group.

**$[\text{Ru}_3(\text{CO})_{12}]$  and Alumina.**—Interaction between (I) and  $\text{Al}_2\text{O}_3$  was carried out in a variety of refluxing hydrocarbon solvents (*n*-pentane, hexane, cyclohexane, *n*-octane, and *n*-nonane). No  $\nu(\text{CO})$  bands were detectable using pentane after 2 h, but the initial spectrum recorded on the orange material formed after 17 h reflux showed sharp bands at  $2062$ ,  $2043$ , and  $1993$   $\text{cm}^{-1}$  superimposed on a broader spectrum. A

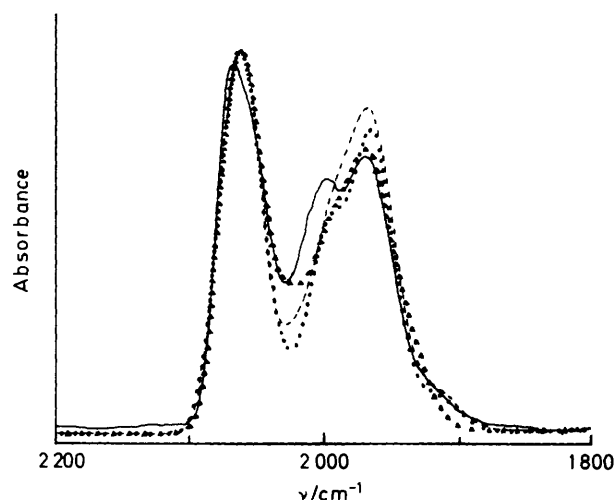
**Table 3.** Spectral parameters used to model the  $^{13}\text{CO}$  (35%) enriched species for the  $[\text{Ru}_3(\text{CO})_{12}]$  and  $\text{TiO}_2$  system

Model	Proportions	Force constants ( $\text{mdyn } \text{\AA}^{-1}$ )	Plotting linewidths ( $\text{cm}^{-1}$ )
(3) ( $\theta = 86^\circ$ ) + (6)	1 : 0.25	(3) $K = 16.71$ $k_1 = 0.62$ (6) $K = 15.52$	(3) $\nu_{\text{sym}}(\text{CO})$ 27 $\nu_{\text{asym}}(\text{CO})$ 36 $\nu(\text{CO})$ 40
(5) ( $\psi = 86^\circ$ ) + (6)	1 : 0.125	(5) $K = 16.65$ $k_{\text{gem}} = 0.54$ $k_{\text{cis}} = 0.057$ $k_{\text{trans}} = 0.078$ (6) $K = 15.32$	(5) 31 (6) 40
(3) ( $\theta = 86^\circ$ ) + (5) ( $\psi = 95^\circ$ )	1 : 0.125	(3) $K = 16.70$ $k_1 = 0.61$ (5) $K = 16.23$ $k_{\text{gem}} = 0.61$ $k_{\text{cis}} = 0.057$ $k_{\text{trans}} = 0.078$	(3) $\nu_{\text{sym}}(\text{CO})$ 27 $\nu_{\text{asym}}(\text{CO})$ 36 (5) 31

**Figure 9.** Background subtracted spectra of the product of  $[\text{Ru}_3(\text{CO})_{12}]$  and  $\text{TiO}_2$  in *n*-octane (20 h): (a) natural abundance and (b)  $^{13}\text{CO}$  enriched

second spectrum recorded immediately after the first only showed the broader bands at 2063s, 2042(sh), 1987s, and 1950m  $\text{cm}^{-1}$ . The reaction was repeated in Schlenk apparatus, but the sharp bands were replaced by broad features at 2037 and 1950  $\text{cm}^{-1}$  which were slowly lost to give a broadened spectrum identical to that described above.

After 25 min reaction time in refluxing hexane, impregn-

**Figure 10.** Modelling studies of the  $\nu(\text{CO})$  bands of the  $^{13}\text{CO}$ -enriched spectrum in Figure 9(b): (—) experimental, (---)  $\text{M}(\text{CO})_2 + \text{M}(\text{CO})$ , (···)  $[\text{M}(\text{CO})_2]_2 + \text{M}(\text{CO})$ , and ( $\blacktriangle\blacktriangle\blacktriangle$ )  $[\text{M}(\text{CO})_2]_2 + \text{M}(\text{CO})_2$ 

ation of (1) onto alumina gave a similar spectrum [2060s, 2045s, 1982s, and 1950(sh)  $\text{cm}^{-1}$ ], although the relative intensity at 2045  $\text{cm}^{-1}$  was greater than in the non-Schlenk pentane reaction. Allowing this sample to remain as a mull in the i.r. spectrometer beam showed the emergence of an absorption at 2030  $\text{cm}^{-1}$ , with the two highest frequency bands merging to one at 2058  $\text{cm}^{-1}$ . Extending the reflux time to 15 h caused broadening of the spectral features, with bands at 2056s, 1983s, and 1950(sh)  $\text{cm}^{-1}$ .

The reaction in cyclohexane gave a pale orange oxide after 45 min with  $\nu(\text{CO})$  absorptions at 2063s, 2046(sh), 1986s, and 1943(sh)  $\text{cm}^{-1}$ . Longer reaction times yielded a broadened spectrum and after 24 h, the reaction solution showed the presence of  $[\text{Ru}_4\text{H}_4(\text{CO})_{12}]$  in addition to the starting material.

Similar treatment in *n*-octane gave a pale brown powder after 70 min with broad  $\nu(\text{CO})$  bands at 2052s, 2033s(sh), 1983s, and 1950(sh)  $\text{cm}^{-1}$ . Extending the reaction time caused further darkening and broadening of the i.r. spectrum (2057 and 1984  $\text{cm}^{-1}$ ). Finally, the oxide recovered from 3.5 h reflux in nonane was pale grey and exhibited a strong i.r. spectrum with bands at 2062m, 2036s, 1985s, and 1949s  $\text{cm}^{-1}$ .

The electronic spectrum of the cyclohexane-produced material, species (L), gave the absorption maxima listed in Table 1. Low-energy bands, possibly due to orbitals of metal-metal character, were observed and there is close agreement with many of the features of the electronic spectrum of species (B) on silica. Comparing the data for these reactions with the work of Zecchina *et al.*<sup>6</sup> shows reasonable agreement between the basic form of the spectra, but the experimental frequencies differ considerably. Species (L) can be described as two components giving rise to  $\nu(\text{CO})$  bands at  $\sim 2063$  and  $1986$  (*cf.*  $2072$  and  $2005$   $\text{cm}^{-1}$ ) and  $2040$  and  $1945$   $\text{cm}^{-1}$  (*cf.*  $2054$  and  $1977$   $\text{cm}^{-1}$ ). According to the previous report these two components are  $\text{Ru}^{\text{II}}(\text{CO})_2$  and  $[\text{Ru}^{\text{II}}(\text{CO})_2]_n$  groups, for the high- and low-frequency pairs respectively. The frequency differences between the two sets of work is not unreasonable due to the variations in preparation and spectroscopic samp-

ling procedures. An additional high-temperature species described in ref. 6 was not produced under our conditions.

### Discussion

A simplified version of the reactions and their products on silica is presented in Figure 11. In agreement with Basset and co-workers,<sup>7</sup> we initially observe  $[\text{Ru}_3(\mu\text{-H})(\text{CO})_{10}(\mu\text{-OSi}\equiv)]$  (2). Air oxidation of (2) afforded a second species (B), which appears to be an oligomer of a  $\text{Ru}(\text{CO})_2$  moiety with a C-Ru-C bond angle of  $\sim 90^\circ$ . A dimeric model gave reasonable intensity agreements with the observed spectrum and preliminary calculations suggested that a cyclic  $\text{Ru}_3(\text{CO})_6$  group would also. The broadness of the  $\nu(\text{CO})$  bands as compared to those observed in a similar study on rhodium carbonyls<sup>8</sup> suggests that (B) may be a mixture of species, perhaps dimers and trimers or higher oligomers; comparison with the  $\nu(\text{CO})$  frequencies of  $[\{\text{Ru}(\text{CO})_2\text{Cl}_3\}_n]$ <sup>12</sup> suggests a +2 oxidation state. This material may be similar to the species (B) observed by Robertson and Webb.<sup>1</sup>

Pyrolysis of (2) however appears to generate a smaller average oligomer of  $\text{Ru}^{\text{II}}(\text{CO})_2$  as species (C), which also corresponds to species (C) in ref. 1, and a small proportion of Ru metal; crystallites have been observed by electron microscopy on a similar material,<sup>7</sup> although one which appears to have contained a higher proportion of metal crystallites. Two remaining species, (D) and (E), giving rise to  $\nu(\text{CO})$  bands at  $2144$  and  $2075$   $\text{cm}^{-1}$ , are considered to be Ru-CO groups. These bands have previously been correlated as part of a  $[\text{Ru}^{\text{II}}(\text{CO})_3]_n$  unit,<sup>7</sup> but our evidence mitigates against this. This is also in agreement with the work of Brown and Gonzalez<sup>13</sup> who observed bands from a 6% Ru/SiO<sub>2</sub> sample at  $2135$  and  $2080$   $\text{cm}^{-1}$  which were both oxygen dependent and not related to each other. High oxidation state ruthenium carbonyl complexes are relatively rare, however  $[\text{Ru}^{\text{III}}(\text{CO})_3\text{F}_3]$  is known and exhibits  $\nu(\text{CO})$  absorptions at  $2148$  and  $2072$   $\text{cm}^{-1}$ .<sup>14</sup> This is likely to represent a high-frequency limit for a  $\text{Ru}^{\text{III}}(\text{CO})_n$  ( $n < 4$ ) site, since a lower value of  $n$  would give less competition for retrodonative bonding. Species (D) and (E) are assigned as  $\text{Ru}^{\text{IV}}(\text{CO})$  and  $\text{Ru}^{\text{III}}(\text{CO})$  sites respectively. Ruthenium(iv) carbonyls are not unknown. Carbonyl stretching frequencies of  $2022$  and  $1970$   $\text{cm}^{-1}$  have been noted for  $\text{Cs}_3[\text{Ru}_2(\text{N})\text{Br}_8(\text{CO})_2]$ .<sup>15</sup> These values are undoubtedly lowered by the strongly  $\pi$ -donating nitride and overall triple negative charge.

The chemistry on the alumina and titania surfaces seems

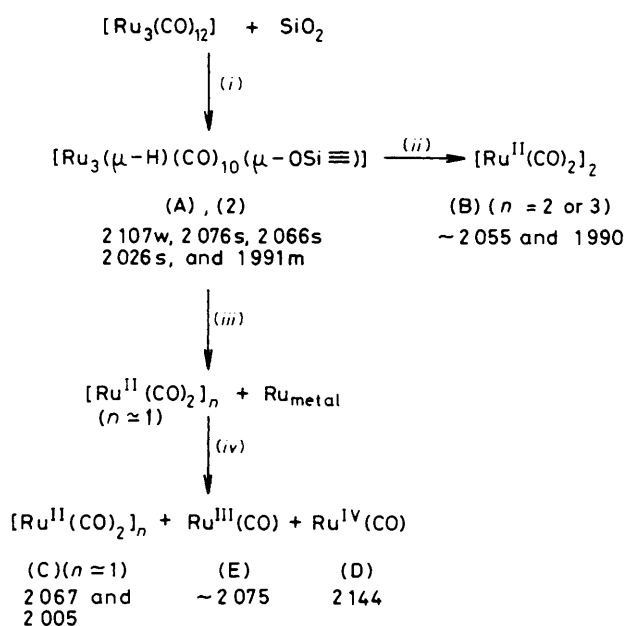


**Figure 11.** Scheme showing reactions of  $[\text{Ru}_3(\text{CO})_{12}]$  on silica and typical  $\nu(\text{CO})/\text{cm}^{-1}$  frequencies of the products; (i) cyclohexane, reflux, 70 min; (ii) air, room temperature; (iii)  $200^\circ\text{C}$ ,  $10^{-1}$  Torr, 15 h; (iv)  $130^\circ\text{C}$ , CO (500 Torr), 24 h

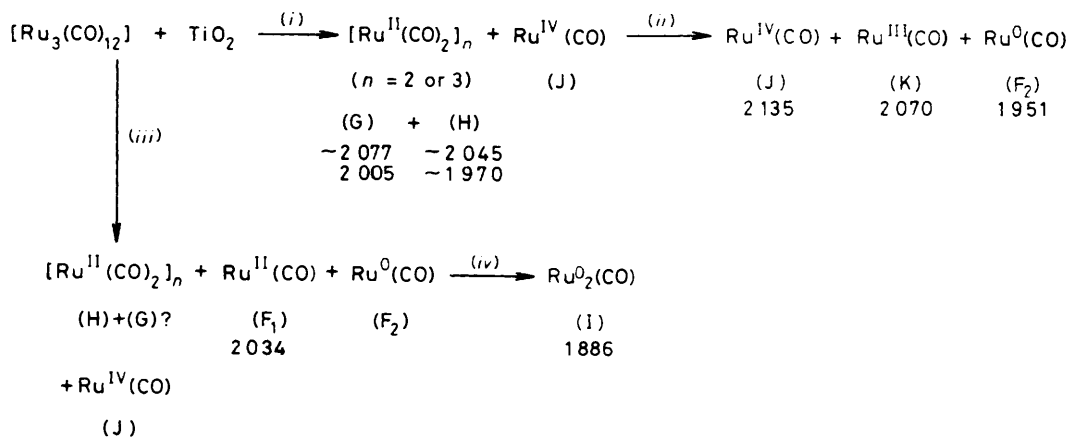


**Figure 12.** Scheme showing reactions of  $[\text{Ru}_3(\text{CO})_{12}]$  on titania and typical  $\nu(\text{CO})/\text{cm}^{-1}$  frequencies of the products; (i) cyclohexane or n-octane, reflux; (ii)  $70^\circ\text{C}$ ,  $10^{-1}$  Torr then CO (300 Torr),  $70^\circ\text{C}$ ; (iii) n-nonane, reflux, 3 h; (iv)  $150^\circ\text{C}$ ,  $10^{-1}$  Torr



very similar, and is related to that on silica. No evidence was obtained for the trinuclear species (2) on these oxides. Previous suggestions as to its formation on alumina<sup>6,16</sup> seem to be due to the superimposition of spectra of other components giving rise to a carbonyl fingerprint somewhat similar to that of (2). Interpretation of the complex chemistry on these surfaces was only possible by observing differential rates of decarbonylation from various sites. However this interpretation is complicated by two competing processes *viz.* changes in the types of ruthenium sites and changes in the degree of hydroxylation and generation of Lewis-acid sites of the oxide itself. This latter effect causes shifts in the frequencies of particular sites through long pyrolysis experiments. A scheme describing the experiments on titania is shown in Figure 12. Two obvious parallels with the silica system are the observations of Ru<sup>IV</sup>-CO [(D) and (J)] and Ru<sup>III</sup>-CO [(E) and (K)] sites. As noted above, the electronic spectra of (B) on SiO<sub>2</sub> and (L) on Al<sub>2</sub>O<sub>3</sub> are very similar. In addition, the i.r. spectra of (G) and (H) on titania are very similar to that of the composite (L) on alumina. Furthermore, the i.r. spectrum of the <sup>13</sup>CO-enriched sample of (B) is close in form to that of these titania-supported species, but the frequencies are lower in the latter case. This suggests that all three oxides generate a mixture of [Ru(CO)<sub>2</sub>]<sub>n</sub> species on the surface under varying conditions of the solution reactions. Reasonable i.r. intensity matches for the dimeric model of SiO<sub>2</sub> and a mixture of dimer and monomer on TiO<sub>2</sub> were obtained. Preliminary calculations on a cyclic trimeric model, however, also seemed viable. The electronic spectral data would also support this. It is therefore proposed that the orange materials consist of a mixture of *cyclo*-Ru<sub>3</sub>(CO)<sub>6</sub> and Ru<sub>2</sub>(CO)<sub>4</sub> groups. Our results, however, cannot eliminate higher oligomers. Species (C) on SiO<sub>2</sub>, which is relatively pale in colour probably consists largely of monomeric Ru(CO)<sub>2</sub> units. An oxidation state of +2 is most probable for all the metal centres in these species.

The relative intensities of the i.r. bands imply that mononuclear species of the type M(CO)<sub>x</sub> (*x* > 2) were not present. Nor were polynuclear species [Ru(CO)<sub>3</sub>X<sub>2</sub>]<sub>n</sub> and [Ru(CO)<sub>4</sub>X<sub>2</sub>]<sub>n</sub> (X = O<sup>-</sup>)<sup>5</sup> evident since simultaneous related intensity changes for more than two bands were not observed. Three other species were noted on the titania surface. Two of these, (F<sub>1</sub>) and (F<sub>2</sub>), had single absorption bands, at ~2 034 and ~1 950 cm<sup>-1</sup> respectively. The former is considered to be a Ru<sup>II</sup>-CO site. The latter has very weak co-ordination to CO and is relatively electron rich. A low oxidation state, possibly metallic site is suggested. A metallic site is also required for species (I) [*ν*(CO) ~1 886 cm<sup>-1</sup>] formed by prolonged pyrolysis at 150 °C. This is evidently a bridging carbonyl. It is interesting to note that only terminal carbonyl groups have been observed by electron energy loss spectroscopy on a clean close-packed ruthenium surface.<sup>17</sup> Indeed since a relatively early observation of a bridging site on a conventionally prepared

silica-supported ruthenium sample,<sup>18</sup> generally terminal sites on metallic and oxidised centres<sup>13,19</sup> have been observed on silica and alumina. Bridging sites have however been reported in the presence of hydrogen.<sup>20</sup>

### Acknowledgements

We wish to thank the S.E.R.C. for a research studentship (to G. S. McN.), Degussa Ltd. for the gift of the oxide samples, and Johnson Matthey Ltd. for the loan of ruthenium chloride.

### References

- 1 J. Robertson and G. Webb, *Proc. R. Soc. London, Ser. A*, 1974, **341**, 383.
- 2 A. F. Simpson and R. Whyman, *J. Organomet. Chem.*, 1981, **213**, 157.
- 3 D. J. Hunt, S. D. Jackson, R. B. Moyes, P. B. Wells, and R. Whyman, *J. Chem. Soc., Chem. Commun.*, 1982, 85.
- 4 H. E. Ferkul, D. J. Stanton, J. D. McCowan, and M. C. Baird, *J. Chem. Soc., Chem. Commun.*, 1982, 955.
- 5 V. L. Kuznetsov, A. T. Bell, and Y. I. Yermakov, *J. Catal.*, 1980, **65**, 374.
- 6 A. Zecchina, E. Guglielminotti, A. Bossi, and M. Camia, *J. Catal.*, 1982, **74**, 225, 240, 252.
- 7 A. Theolier, A. Choplin, L. D'Ornelas, J. M. Basset, G. Zanderighi, R. Ugo, P. Psaro, and C. Sourisseau, *Polyhedron*, 1983, **2**, 119.
- 8 J. Evans and G. S. McNulty, *J. Chem. Soc., Dalton Trans.*, 1984, 587.
- 9 G. Collier, D. J. Hunt, S. D. Jackson, R. B. Moyes, I. A. Pickering, P. B. Wells, A. F. Simpson, and R. Whyman, *J. Catal.*, 1983, **20**, 154.
- 10 D. R. Tyler, R. A. Levenson, and H. B. Gray, *J. Am. Chem. Soc.*, 1978, **100**, 7888.
- 11 C. R. Eady, P. F. Jackson, B. F. G. Johnson, J. Lewis, M. C. Malatesa, M. McPartlin, and W. J. H. Nelson, *J. Chem. Soc., Dalton Trans.*, 1980, 383.
- 12 M. J. Cleare and W. P. Griffith, *J. Chem. Soc. A*, 1969, 372.
- 13 M. F. Brown and R. D. Gonzalez, *J. Phys. Chem.*, 1976, **80**, 1731.
- 14 A. J. Hewitt, J. H. Holloway, R. D. Peacock, J. B. Raynor, and I. L. Wilson, *J. Chem. Soc., Dalton Trans.*, 1976, 579.
- 15 W. P. Griffith and D. Pawson, *J. Chem. Soc., Dalton Trans.*, 1973, 1315.
- 16 J. Evans and B. P. Gracey, *J. Chem. Soc., Dalton Trans.*, 1982, 1123.
- 17 G. E. Thomas and W. H. Weinberg, *J. Chem. Phys.*, 1979, **70**, 1437.
- 18 C. R. Guerra and J. H. Schulman, *Surf. Sci.*, 1967, **7**, 229.
- 19 R. A. Dalla Betta, *J. Phys. Chem.*, 1975, **79**, 2519.
- 20 K. Fujimoto, M. Kameyama, and T. Kunugi, *J. Catal.*, 1980, **61**, 7.

Received 5th July 1983; Paper 3/1161